

Hamiltonian Flow in Coulomb Gauge Yang-Mills Theory

Markus Leder,¹ Jan M. Pawłowski,^{2,3} Hugo Reinhardt,¹ and Axel Weber⁴

¹*Institut für Theoretische Physik, Universität Tübingen,
Auf der Morgenstelle 14, 72076 Tübingen, Germany*

²*Institut für Theoretische Physik, Universität Heidelberg, Philosophenweg 16, 62910 Heidelberg, Germany*

³*ExtreMe Matter Institute EMMI, GSI Helmholtzzentrum für Schwerionenforschung,
Planckstr. 1, 64291 Darmstadt, Germany*

⁴*Instituto de Física y Matemáticas, Universidad Michoacana de San Nicolás de Hidalgo,
Edificio C-3, Ciudad Universitaria, 58040 Morelia, Michoacán, Mexico*

(Dated: September 1, 2018)

We derive a new functional renormalization group equation for Hamiltonian Yang-Mills theory in Coulomb gauge. The flow equations for the static gluon and ghost propagators are solved under the assumption of ghost dominance within different diagrammatic approximations. The results are compared to those obtained in the variational approach and the reliability of the approximations is discussed.

PACS numbers: 12.38.Aw, 05.10.Cc, 11.10.Ef, 11.15.Tk

I. INTRODUCTION

QCD is experimentally well-tested as the theory of strong interactions in the perturbative regime where asymptotic freedom holds. In the non-perturbative regime we have collected much theoretical evidence ranging from a linearly rising potential for heavy quarks to hadronic observables which match at least qualitatively the experimental values. These non-perturbative results were either obtained by lattice methods, QCD-model computations and in recent years, to an increasing extent, by first principle continuum QCD computations based on functional methods. Despite the impressive success of these combined efforts there still remains much to be understood, both qualitatively and quantitatively. Open physics questions range from the mechanism of confinement and its relation to spontaneous chiral symmetry breaking to the properties of QCD at finite temperature and density. Progress in these directions can only be obtained with a combination of the methods at hand, in particular, when it comes to the understanding of the underlying physics mechanisms.

This has triggered an increasing interest in non-perturbative studies of continuum Yang-Mills theory and full QCD in recent years. Many of these studies were carried out in Landau gauge, using Dyson-Schwinger equations (DSE), for reviews see [1–5] (see also [6]), as well as the functional renormalization group (FRG) equations, for reviews see [7–9] (see also [10]). Another attractive possibility is Coulomb gauge, which has been pursued either with DSEs, e.g. [11–13], or with a variational approach to the Hamiltonian formulation [14–19], for a short introduction see [20]. Each approach has its own advantages and drawbacks and by combining the different approaches one can expect to gain new insights into the theory, in particular, into the non-perturbative regime.

In this spirit we put forward in the present paper a functional renormalization group approach to the Hamil-

tonian formulation of Yang-Mills theory. A specific advantage of the Hamiltonian formulation is its close connection to physics as demonstrated in various applications, see e.g. [21]. However, Hamiltonian renormalization is a well-known non-trivial task which has hampered progress in the Hamiltonian approach for many years. Specifically it complicates the search for RG-invariant, self-consistent approximations to the full vacuum wave functional. In the present Hamiltonian FRG approach to Coulomb gauge Yang-Mills theory the latter task is directly solved by a self-consistent approximation to the flow equation. Such a procedure guarantees RG invariance by its very definition, and hence combines the advantages of the Hamiltonian approach with that of the FRG. We will also show explicitly that with suitable truncations the integrated flow equations become precisely the DSEs of the variational approach [15] with a Gaussian ansatz for the vacuum wave functional. In our explicit computations we will focus on the infrared sector of the theory within the ghost-dominance scenario. Therefore we only include full momentum-dependent gluon and ghost propagators and the bare ghost-gluon vertex. The latter approximation is justified by the non-renormalization of the full ghost-gluon vertex.

The paper is organized as follows: In section II we present the basics of the functional renormalization group (FRG) flow equation approach. In particular, we derive the flow equation for the Hamiltonian approach to Yang-Mills theory in Coulomb gauge. The gauge fixing in the scalar product of the wave functional is accomplished by the Faddeev-Popov method. In section III the FRG flow equations for the gluon and ghost propagators are derived assuming a bare, non-running, ghost-gluon vertex. We also extend the uniqueness proof for the infrared scaling solution in Landau gauge to Coulomb gauge Yang-Mills theory. In sect. IV we numerically solve the flow equations for ghost and gluon propagators within two different approximations which are compared with the DSE results. Finally our conclusions are given in sect.

V. Some mathematical details of the derivation of the flow equations of the Hamiltonian approach as well as some details of the numerical procedure are deferred to the appendices.

II. DERIVATION OF THE HAMILTONIAN FLOWS

A. Flow equation for the effective action

Below we briefly summarize the essential ingredients of the FRG approach. The starting point is the finite renormalized generating functional of the Green's functions,

$$Z[j] = \int [D\varphi]_{\text{ren}} e^{-S[\varphi] + j \cdot \varphi}, \quad (1)$$

where the subscript “ren” of the measure indicates an appropriate renormalization procedure that renders the functional integral in (1) finite, for more details see [8]. Here φ and j denote collectively all fields involved and the corresponding sources. Furthermore, the scalar product $j \cdot \varphi$ includes summation over all indices and integration over space-time. Finally, the theory is specified by the classical action $S[\varphi]$ and the renormalized functional integral measure. In the functional renormalization group (FRG) approach the generating functional is IR regularized by adding a regulator term ΔS_k to the classical action S . It depends on a cut-off momentum k and is chosen to be quadratic in the fields,

$$\Delta S_k[\varphi] = \frac{1}{2} \varphi \cdot R_k \cdot \varphi \equiv \frac{1}{2} \int \frac{d^d p}{(2\pi)^d} \varphi(-p) R_k(p) \varphi(p). \quad (2)$$

The regulator function $R_k(p)$ is an effective momentum dependent mass and has the properties

$$\begin{aligned} \lim_{p/k \rightarrow 0} R_k(p) &> 0 \\ \lim_{k/p \rightarrow 0} R_k(p) &= 0. \end{aligned} \quad (3)$$

The first condition ensures that $R_k(p)$ is indeed an infrared regulator and suppresses the propagation of the modes with momentum $p \lesssim k$. The second condition implies that the momentum modes with $p \gg k$ are unaffected by the regulator and that the full finite renormalized generating functional of the theory at hand is recovered as the cut-off scale k is pushed to zero.

The basic idea of the FRG flow equation approach to Yang-Mills theory is to start at a large cut-off scale k , where the theory is under control due to asymptotic freedom, and then let the cut-off k flow to the small momentum regime, which is non-perturbative. The evolution of the Green's functions with the cut-off scale k is described by a flow equation which is obtained by taking the derivative of the regulated generating functional

$$Z_k[j] = \int [D\varphi]_{\text{ren}} e^{-S[\varphi] - \Delta S_k[\varphi] + j \cdot \varphi} \equiv e^{W_k[j]} \quad (4)$$

w.r.t. the momentum scale k . We also remark that the finiteness of $Z_k[j]$ follows from that of $Z[j]$ with the representation

$$Z_k[j] = e^{-\Delta S_k[\delta/\delta j]} Z[j] \quad (5)$$

and the differentiability of $Z[j]$ w.r.t. j . With (5) the flow of Z_k is derived as

$$\partial_t Z_k[j] = \left(-\frac{1}{2} \frac{\delta}{\delta j} \cdot \dot{R}_k \cdot \frac{\delta}{\delta j} \right) Z_k[j], \quad (6)$$

where the dot on R stands for the derivative w.r.t. the dimensionless variable $t = \ln k/k_0$. Here k_0 is an arbitrary reference scale. The functional derivative $\delta/\delta j$ in momentum space is to be understood as

$$\frac{\delta}{\delta j}(p) \equiv (2\pi)^d \frac{\delta}{\delta j(-p)}. \quad (7)$$

Expressing (6) in terms of the generating functional of the connected Green's functions, $W_k[j]$, defined in (4), we get

$$\partial_t W_k[j] = -\frac{1}{2} \frac{\delta W_k}{\delta j} \cdot \dot{R}_k \cdot \frac{\delta W_k}{\delta j} - \frac{1}{2} \text{Tr} \dot{R}_k \frac{\delta^2 W_k}{\delta j \delta j}, \quad (8)$$

where

$$\text{Tr} \dot{R}_k \frac{\delta^2 W_k}{\delta j \delta j} \equiv \int \frac{d^d p}{(2\pi)^d} \dot{R}_k(p) (2\pi)^{2d} \frac{\delta^2 W_k}{\delta j(-p) \delta j(p)}. \quad (9)$$

By taking derivatives of (8) w.r.t. j one obtains the flow equations for the connected Green's functions. In practice, it is usually more convenient to perform first a Legendre transform from the sources j to the classical field

$$\phi = \frac{\delta W_k[j]}{\delta j}, \quad (10)$$

resulting in the effective action

$$\Gamma_k[\phi] = (-W_k[j] + j \cdot \phi)_{j=j_k(\phi)} - \frac{1}{2} \phi \cdot R_k \cdot \phi, \quad (11)$$

where $j_k(\phi)$ is given by solving (10) for j . Hence, (11) also implies that

$$j = \frac{\delta(\Gamma_k + \Delta S_k)}{\delta \phi}. \quad (12)$$

By taking the derivative of the effective action Γ_k w.r.t. $t = \ln k/k_0$ and using its definition (11) and (8) one arrives at

$$\partial_t \Gamma_k[\phi] = \frac{1}{2} \text{Tr} \dot{R}_k \frac{\delta^2 W_k}{\delta j \delta j}. \quad (13)$$

The second derivative of W_k w.r.t. the currents is the connected two-point function, the propagator of the theory. It is related to the inverse of the second derivative of the effective action,

$$\frac{\delta^2 W_k}{\delta j \delta j} = \left(\frac{\delta^2 \Gamma_k}{\delta \phi \delta \phi} + R_k \right)^{-1}. \quad (14)$$

Eq. (14) follows directly from (12) and

$$\frac{\delta}{\delta\phi} j = \left(\frac{\delta}{\delta j} \phi \right)^{-1} = \left(\frac{\delta^2 W_k}{\delta j \delta j} \right)^{-1}. \quad (15)$$

Inserting (14) into (13) we obtain Wetterich's flow equation for the effective action [22],

$$\dot{\Gamma}_k[\phi] = \frac{1}{2} \text{Tr} \dot{R}_k \left(\Gamma_k^{(2)}[\phi] + R_k \right)^{-1}, \quad (16)$$

where the dot denotes the derivative w.r.t. t and

$$\Gamma_{k,1\dots n}^{(n)}[\phi] = \frac{\delta^n \Gamma_k[\phi]}{\delta\phi_1 \dots \delta\phi_n} \quad (17)$$

are the one-particle irreducible n -point functions (proper vertices). We have also introduced a condensed notation where n stands for the space-time variable, $\phi_n = \phi(x_n)$. The generic structure of this equation is independent of the details of the underlying theory, i.e., of the explicit form of the action $S[\phi]$, but is a mere consequence of the form of the regulator term (2), i.e., that it is quadratic in the fields. By taking functional derivatives of Eq. (16) w.r.t. the fields one obtains the flow equations for the (inverse) propagators or vertices. Taking the second functional derivative we find the flow equation for the two-point function,

$$\dot{\Gamma}_{k,12}^{(2)} = \frac{1}{2} \text{Tr} \dot{R}_k \left(\Gamma_k^{(2)}[\phi] + R_k \right)^{-1} \left(-\Gamma_{k,12}^{(4)} + \left[\Gamma_{k,1}^{(3)} \left(\Gamma_k^{(2)}[\phi] + R_k \right)^{-1} \Gamma_{k,2}^{(3)} + (1 \leftrightarrow 2) \right] \right) \left(\Gamma_k^{(2)}[\phi] + R_k \right)^{-1}. \quad (18)$$

In (18) we have suppressed all cyclic indices, which are summed (integrated) over in the trace. The flow equation (18) for the propagator is diagrammatically illustrated in Fig. 1.

B. Hamiltonian flows

In this section we derive the flow equation for the effective action in the Hamiltonian approach. Some details can be found in Appendix A. In the Hamiltonian approach the generating functional of the static (equal-time) Green's functions is defined by

$$Z[j] = \langle \psi | \exp(j \cdot \varphi) | \psi \rangle = \int \mathcal{D}\varphi |\psi[\varphi]|^2 \exp(j \cdot \varphi), \quad (19)$$

where $\langle \varphi | \psi \rangle = \psi[\varphi]$ is the vacuum wave functional. Comparison with Eq. (1) shows that in the Hamiltonian approach the “action” is defined by the wave functional

$$\exp(-S[\varphi]) \equiv |\psi[\varphi]|^2. \quad (20)$$

With this identification Eq. (19) has precisely the standard form of the generating functional (1), except that the functional integral extends over time-independent fields, and we can repeat, step by step, the formal manipulations of the last section to derive the corresponding FRG flow equation, which has the same structure as Eq. (16).

In the present work we are specifically interested in the Hamiltonian flow of Yang-Mills theory in Coulomb gauge. In this case φ stands for the transverse spatial components of the gauge field A ,

$$t_{ij} A_j = A_i \quad \text{with} \quad t_{ij}(\mathbf{p}) = \delta_{ij} - \frac{p_i p_j}{\mathbf{p}^2}. \quad (21)$$

Note that in the present Hamiltonian context, we denote the contravariant components of all 3-vectors with subscripts. The wave functional $\psi(A)$ is the true Yang-Mills vacuum wave functional restricted to transverse fields. Implementing the Coulomb gauge in the standard fashion by the Faddeev-Popov method, the generating functional (19) reads

$$Z[J] = \int \mathcal{D}A \det(-\partial D) |\psi[A]|^2 \exp(J \cdot A), \quad (22)$$

where $\det(-\partial D)$ denotes the Faddeev-Popov determinant and

$$D^{ab} = \delta^{ab} \partial + g f^{acb} A^c, \quad (23)$$

is the covariant derivative in the adjoint representation. The short hand notation $J \cdot A$ also includes the internal indices,

$$J \cdot A = \int \frac{d^3 p}{(2\pi)^3} J_i^a(-\mathbf{p}) A_i^a(\mathbf{p}). \quad (24)$$

The Faddeev-Popov determinant $\det(-\partial D)$ is represented by an integral over ghost fields $c^a(\mathbf{x})$, $\bar{c}^a(\mathbf{x})$. After introducing regulator terms for ghosts and gluons via ΔS_k , see Eq. (2), the regulated generating functional (4) of the Hamiltonian approach to Yang-Mills theory in Coulomb gauge reads

$$\begin{aligned} Z_k[J, \sigma, \bar{\sigma}] &= \int \mathcal{D}A \mathcal{D}\bar{c} \mathcal{D}c e^{-S - \Delta S_k + J \cdot A + \bar{\sigma} \cdot c + \bar{c} \cdot \sigma} \\ &\equiv \exp W_k[J, \sigma, \bar{\sigma}]. \end{aligned} \quad (25)$$

The “classical action” S in (25) is given by

$$S = -\ln |\psi[A]|^2 + \int d^3 x \bar{c}^a(\mathbf{x}) (-\partial D)^{ab} c^b(\mathbf{x}) \quad (26)$$

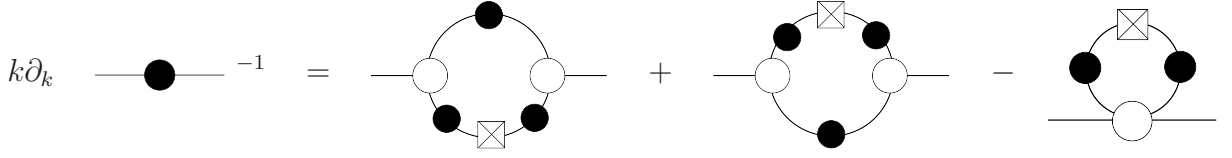


FIG. 1: Flow equation for the inverse propagator (2-point function) $\Gamma_k^{(2)} = \langle \phi \phi \rangle^{-1}$. Here and in all the diagrammatic equations below, lines with full circles represent $(\Gamma_k^{(2)} + R_k)^{-1}$ on the r.h.s. of the equation, but only $\Gamma_k^{(2)-1}$ on its l.h.s. Open circles represent full proper vertices $\Gamma_k^{(n)}$, while the square with a cross represents the regulator insertion \dot{R}_k .

and the regulator term is chosen as

$$\Delta S_k[A, c, \bar{c}] = \frac{1}{2} A \cdot R_{A,k} \cdot A + \bar{c} \cdot R_{c,k} \cdot c. \quad (27)$$

Here we have used again the short hand notation for scalar products, e.g.

$$A \cdot R_{A,k} \cdot A = \int \frac{d^3 p}{(2\pi)^3} A_i^a(-\mathbf{p}) R_{A,k}^{ab}(\mathbf{p}) A_i^b(\mathbf{p}). \quad (28)$$

In (28) the transversality of the gauge field, $A_i^a(\mathbf{p}) = t_{ij}(\mathbf{p}) A_j^a(\mathbf{p})$, is implied. Put differently, we could have multiplied the regulator with the transverse projector. Due to global color symmetry and spatial rotational symmetry, the regulators take the form

$$\begin{aligned} R_{A,k}^{ab}(\mathbf{p}) &= R_{A,k}(p) \delta^{ab}, \\ R_{c,k}^{ab}(\mathbf{p}) &= R_{c,k}(p) \delta^{ab}, \end{aligned} \quad (29)$$

with the notation $p = |\mathbf{p}|$ that we shall use from now on. Both regulators are chosen to depend on the same dimensionless shape function $r_k(p)$. Accounting for dimensions we put

$$\begin{aligned} R_{A,k}(p) &= 2p r_k(p), \\ R_{c,k}(p) &= g p^2 r_k(p) = g \bar{R}_{c,k}(p). \end{aligned} \quad (30)$$

(see our remarks following Eq. (50) concerning the factor g included in the definition of $R_{c,k}(p)$). In the numerical solution we have chosen the $r_k(p)$ as given in (57).

From the regularized generating functional (25) one derives the flow equation for the effective action as outlined in the previous section for a single field. In the present case, for compactness of the notation, it is convenient to combine gluon and ghost fields into a superfield

$$\varphi = (A, c, \bar{c}), \quad \bar{\varphi} = (A, -\bar{c}, c). \quad (31)$$

Accordingly, we introduce the supersources

$$I = (J, \sigma, \bar{\sigma}), \quad \bar{I} = (J, -\bar{\sigma}, \sigma) \quad (32)$$

and supermatrices

$$\begin{aligned} \mathcal{R}_k &= \text{diag}(R_{A,k}, R_{c,k}, R_{c,k}^T) \\ M &= \text{diag}(\mathbf{1}, -\mathbf{1}, -\mathbf{1}), \end{aligned} \quad (33)$$

where M figures as metric in the superspace and enters the definition of the supertrace,

$$\text{STr}(\dots) \equiv \text{Tr}(M \dots). \quad (34)$$

With this notation the effective action (11) is given by

$$\Gamma_k[\phi] = -W_k[I_k] + I_k \cdot \bar{\phi} - \frac{1}{2} \bar{\phi} \cdot \mathcal{R}_k M \cdot \phi, \quad (35)$$

where $W_k[I_k]$ is defined by Eq. (25) and

$$\bar{\phi} = \frac{\delta W_k[I_k]}{\delta I_k} \quad (36)$$

is the classical superfield $\phi = \langle \varphi \rangle$ with $\phi = (A, c, \bar{c})$, where in a slight abuse of notation we use the same symbols for the components of ϕ and φ . The flow of the effective action reads (cf. Eq. (13))

$$\partial_t \Gamma_k[\phi] = \frac{1}{2} \text{STr} \mathcal{R}_k \frac{\delta^2 W_k}{\delta \bar{I} \delta I}. \quad (37)$$

By means of (36) one derives from (35) (cf. Eq. (14))

$$\frac{\delta^2 W_k}{\delta \bar{I} \delta I} = \left(\frac{\delta^2 \Gamma_k}{\delta \bar{\phi} \delta \phi} + \mathcal{R}_k \right)^{-1} \quad (38)$$

and obtains the desired flow equation (cf. Eq. (16))

$$\partial_t \Gamma_k = \frac{1}{2} \text{STr} \dot{\mathcal{R}}_k \left(\Gamma_k^{(2)} + \mathcal{R}_k \right)^{-1}, \quad (39)$$

where $\Gamma_k^{(2)} = \delta^2 \Gamma_k / \delta \bar{\phi} \delta \phi$. In the present Hamiltonian approach to Yang-Mills theory in Coulomb gauge the effective action $\Gamma_k[\phi]$ defined by Eqs. (25), (26) and (35) is exclusively determined by the vacuum wave functional $\psi[A]$ and the Faddeev-Popov determinant. Importantly, the FRG approach does not require the knowledge of the full vacuum wave functional. It is sufficient to know the wave functional in the asymptotic region $k \rightarrow \infty$, where perturbation theory applies. The full quantum effective action $\Gamma_{k \rightarrow 0}$ and hence the full vacuum wave functional is then computed by solving the flow equation, making suitable ansätze and truncations for Γ_k or its derivatives.

III. FLOWS FOR COULOMB GAUGE YANG MILLS THEORY

A. Uniqueness of IR scaling

The Hamiltonian flow equation set up for Coulomb gauge Yang-Mills theory in the last section IIB very much resembles the one in Landau gauge, but in one dimension less. It has already been speculated that there is a close connection between these two formulations, [23]. Here we shall employ the similarities in order to derive unique scaling laws for the infrared behavior of Coulomb gauge Yang-Mills theory.

It has been shown in [24, 25] that Landau gauge Yang-Mills theory admits a unique infrared scaling solution [26]. Moreover, this solution implies ghost dominance. We emphasize that uniqueness refers to the unique scaling relations if scaling is present. Indeed, Landau gauge Yang-Mills theory also admits a solution without such a scaling behavior, the decoupling solution. More details can be found e.g. in [1]. The scaling and decoupling solutions also exist for the DSE obtained in the Hamiltonian formulation of Yang-Mills theory in Coulomb gauge and were baptized “critical” and “subcritical” solutions [19]. Furthermore, lattice calculations [23] show that the scaling or critical solution is realized in Coulomb gauge.

The proof in [24] was based on the comparison of the full hierarchies of DSE and FRG equations for Green’s functions. Apart from this it only relied on the details of the coupling between ghosts and gluons and the canonical scaling properties of the gluonic self-coupling. This has been made transparent in [24]. The proof as formulated there can be directly transferred to Coulomb gauge, the only missing piece is provided by the flow equation derived in the present work.

With the Hamiltonian Coulomb gauge DSEs and the FRGs we derive the same set of constraint equations for the scaling coefficients as in [24]. There are additional terms coming from the higher classical gluonic n -point vertices which all can be proven to be sub-leading. This relates to the fact that the canonical scaling of classical gluonic vertices is less divergent than that of the dressed vertices. In summary we conclude that also Coulomb gauge in its Hamiltonian formulation admits a unique scaling solution with the same scaling laws that are satisfied in Landau gauge in $d = 3$. The scaling relations relevant for the present work are that for the propagators,

$$\langle A(p)A(-p) \rangle \propto \frac{1}{p^{2(1+\kappa_A)}}, \quad \langle c(p)\bar{c}(-p) \rangle \propto \frac{1}{p^{2(1+\kappa_c)}}, \quad (40)$$

and for the ghost gluon vertex at the symmetric point,

$$\frac{\delta^3 \Gamma_k}{\delta \bar{c}^a \delta c^b \delta A_i^c} \propto p^{2\kappa_{\bar{c}cA}} \frac{\delta^3 S}{\delta \bar{c}^a \delta c^b \delta A_i^c}. \quad (41)$$

The scaling solution entails the non-renormalization of the ghost-gluon vertex, $\kappa_{\bar{c}cA} = 0$, and a scaling relation

for the scaling of the ghost and gluon propagator, summarized as

$$\kappa_{\bar{c}cA} = 0 \quad \text{and} \quad \kappa_A = -\frac{1}{2} - 2\kappa_c, \quad \text{with} \quad \kappa_A \leq -\frac{1}{4}. \quad (42)$$

Eq. (42) implies ghost-dominance in the sense that diagrams with ghost lines dominate in the infrared over diagrams with gluonic lines, see also [24]. The scaling coefficients α, β used in Coulomb gauge are defined via

$$\langle A(p)A(-p) \rangle \propto p^\alpha, \quad \langle c(p)\bar{c}(-p) \rangle \propto \frac{1}{p^{2+\beta}}, \quad (43)$$

see Eq. (58) below. The coefficients α and β relate to the κ ’s via $\alpha = -2 - 2\kappa_A$ and $\beta = 2\kappa_c$. Hence we find *unique* scaling laws in Coulomb gauge with the scaling relation

$$\alpha = 2\beta - 1. \quad (44)$$

The sum rule (44) has been found in DSE analyses in Coulomb gauge before [17], here we have proven its uniqueness.

B. Propagator flows

The propagator flows are obtained from the flow equation for the effective action (39) by differentiating twice w.r.t. the fields. These derivations are detailed in Appendix B, their outcome is represented diagrammatically in Figs. 2, 3. All propagators and vertices, denoted by black and white circles respectively, are fully dressed k -dependent correlation functions. This has to be compared with DSE equations for the propagators where all diagrams contain one bare vertex.

For a solution of these equations we have to approximate the full effective action. In the present work we approximate it by the classical action and fully momentum dependent (inverse) propagators. We are specifically interested in the infrared where we assume scaling. Uniqueness of scaling as proven in the last section III A then implies ghost dominance. Consequently, we drop the gluonic vertices and only keep the ghost vertices. The resulting flow equations for the gluon and ghost propagators are shown in Figs. 4, 5.

We pause here for a moment to discuss the meaning of and the justification for this truncation in detail. The generating functional (22) is a functional integral defined by the full vacuum wave functional $\psi[A]$ which is, however, unknown. In Ref. [27], the vacuum functional has been determined explicitly to one-loop order through a perturbative solution of the Schrödinger equation for the Christ-Lee Hamiltonian. It was found that non-local terms in the couplings of two, three and four gluon fields in the wave functional give contributions to the static gluon propagator that are relevant to its ultraviolet behavior, in particular its anomalous dimension. In higher loop orders, non-local terms in the couplings of more than

FIG. 2: Flow equation of the gluon propagator, Eq. (B9). Here and in the following, the spiral and dotted lines with the black circles denote the regularized gluon and ghost propagators at cutoff momentum k , respectively. White circles stand for proper vertices at cutoff k , a regulator insertion \hat{R}_k is represented by a square with a cross.

FIG. 3: Flow equation of the ghost propagator, Eq. (B8)

four gluon fields will also become relevant to the gluon two-point function. By non-local we refer to coefficient functions that become singular for exceptional momenta. By neglecting these terms in the truncation considered in the present paper, the ultraviolet behavior of the two-point function will not be accurately reproduced, i.e., the power of the logarithmic correction in this kinematic regime will be incorrect.

On the other hand, such non-local terms and three- and four-gluon couplings are not necessarily relevant to the infrared behavior, which is our main concern here: it has been argued [28] that in the infrared the static ghost propagator is strongly enhanced relative to its tree level behavior, while the gluon propagator is suppressed or even vanishing. This is precisely what happens for the unique scaling solution as discussed in the previous section: the infrared behavior is dominated by those diagrams with the largest number of ghost propagators (“ghost dominance”). Indeed, the arguments about the kinematic singularities in [24] can also be directly transferred to Coulomb gauge. They entail that for the scaling solution neither the non-local terms described before nor the couplings of three or more gluons in general contribute to those diagrams that dominate the infrared behavior. The same can be inferred from the diagrammatic analysis of Ref. [27] when extended to higher perturbative orders, if one takes into account that there are no non-local terms or higher couplings including ghost fields in the “action” (26).

The approximation of keeping a bare or tree-level ghost-gluon vertex is based on the “non-renormalization theorem” for this vertex [29]. Although this theorem was originally formulated for QCD in Landau gauge and the space-time correlation functions, the argument carries over without change to the present situation. Indeed

we have shown in the last section that it follows for the unique scaling solution. It has been confirmed on the non-perturbative level for the Landau gauge case in lattice studies [30]. As for the Coulomb gauge, a perturbative evaluation of the vertex (to one-loop level) at the symmetric point shows that the quantum corrections are finite and independent of the scale [27, 31].

In summary, we can drop the gluonic vertices in the infrared without spoiling the quantitative nature of our approximation. We emphasize that for large momenta this is evidently not true. Finally, we also drop the tadpole diagrams in the flow equations for the static propagators. The four-point couplings appearing in these diagrams are not contained in the integrand of the generating functional, but can build up in the course of the renormalization group flow. We simply assume that their contribution is negligible in the infrared, at least for the qualitative behavior of the two-point correlation functions, which leads us to the final form of the flow equations represented in Figs. 4, 5.

IV. EFFECTIVE ACTION AND FLOWS

A. Parametrization of the effective action

The arguments above single out a specific approximation of the effective action. First of all, it relies on an expansion of the effective action in powers of the field,

$$\Gamma_k[\phi] = \sum_{N_A, N_c, N_{\bar{c}}} \frac{1}{N_A!} \frac{1}{N_c!} \frac{1}{N_{\bar{c}}!} \Gamma_{k, n_1 \dots n_N}^{(N)} \cdot \phi_{n_1} \dots \phi_{n_N}, \quad (45)$$

where the ϕ_{n_i} stand for either the gluon fields ($\phi = A$) or the ghost fields ($\phi = c, \bar{c}$). In the following we take into

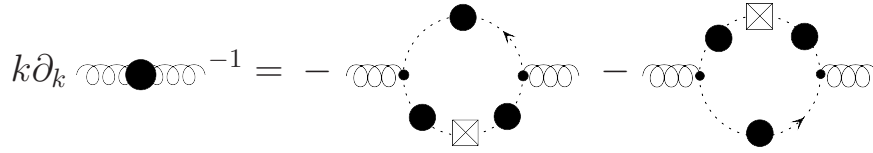


FIG. 4: Truncated flow equation of the gluon propagator. Here and in the following, the bare vertices at $k = \Lambda$ are symbolized by small dots.

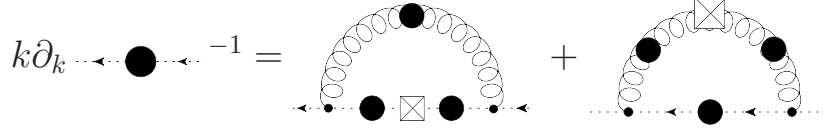


FIG. 5: Truncated flow equation of the ghost propagator.

account the bare ghost-gluon vertex and the full momentum dependent propagators. In an upgrade of the approximation we will also take into account tadpole terms related to ghost and ghost-gluon vertices. This provides a first error estimate for the approximation scheme set up here. All other vertices are set to zero. Therefore, in the minimal order of the approximation the only non-vanishing n -point functions are the ghost and gluon (inverse) propagators and the ghost-gluon vertex.

We parametrize the inverse gluon propagator as follows,

$$(2\pi)^6 \frac{\delta^2 \Gamma_k}{\delta A_i^a(\mathbf{p}) \delta A_j^b(\mathbf{q})} = \delta^{ab} t_{ij}(\mathbf{p}) 2\omega_k(p) (2\pi)^3 \delta^3(\mathbf{p} + \mathbf{q}). \quad (46)$$

The diagonality in color space is due to global color symmetry. The transverse projector comes with the choice of Coulomb gauge where the gauge fields are transverse, see (21), and momentum conservation arises from spatial translational invariance of the theory. The only quantity left to be determined by the flow equation is $\omega_k(p)$, which depends only on the absolute value of the external momentum due to rotational invariance of the theory, and on the cutoff momentum k . The factor of 2 is mere convention. In the flow we need the gluon propagator $G_{A,k} t_{ij} \delta^{ab}$ with the scalar function

$$G_{A,k}(p) = \frac{1}{2\omega_k(p) + R_{A,k}(p)}. \quad (47)$$

The full gluon propagator at vanishing cut-off is given by $G_A(p) = 1/2\omega(p)$, with $\omega(p) \equiv \omega_0(p)$. The ghost two-point function can be expressed as

$$-(2\pi)^6 \frac{\delta^2 \Gamma_k}{\delta \bar{c}^a(\mathbf{p}) \delta c^b(\mathbf{q})} = \delta^{ab} g \frac{p^2}{d_k(p)} (2\pi)^3 \delta^3(\mathbf{p} + \mathbf{q}), \quad (48)$$

where $d_k(p)$ is the ghost form factor, which is the quantity to be calculated. The ghost propagator $G_{c,k} \delta^{ab}$ comprises the scalar function

$$G_{c,k}(p) = \frac{1}{g} \bar{G}_{c,k}(p) \quad (49)$$

with

$$\bar{G}_{c,k}(p) = \frac{1}{p^2/d_k(p) + \bar{R}_{c,k}(p)}. \quad (50)$$

We have included an explicit constant factor of $1/g$ in the definition of the ghost form factor for ease of comparison with the Dyson-Schwinger equations of the variational approach in subsection IV C. The full ghost propagator at vanishing cut-off is $G_c(p) = d(p)/gp^2$, where $d(p) \equiv d_0(p)$. The last quantity to specify is the ghost-gluon vertex. We have argued in the previous section that it is well approximated by its bare part,

$$\begin{aligned} -(2\pi)^9 \frac{\delta^3 \Gamma_k}{\delta \bar{c}^a(\mathbf{p}_1) \delta c^b(\mathbf{p}_2) \delta A_i^c(\mathbf{p}_3)} = \\ -ig f^{abc} p_{1,j} t_{ij}(\mathbf{p}_3) (2\pi)^3 \delta^3(\mathbf{p}_1 + \mathbf{p}_2 + \mathbf{p}_3), \end{aligned} \quad (51)$$

where we have used the fact that the gauge field is transverse in Coulomb gauge. With these conventions, in particular Eq. (48), a suitable choice of the renormalization group invariant coupling g_R is

$$g_R(p) = d(p)(p/\omega(p))^{1/2}, \quad (52)$$

see [32].

B. Approximation without tadpoles

Now we are in the position to solve the flow equations for the propagators within the minimal truncation introduced above: the only non-vanishing vertex function is the bare ghost-gluon vertex (51). In particular this eliminates the tadpole diagrams. Inserting this approximation into the flow equations for the gluon and ghost propagators shown in Figs. 4, 5 we arrive at

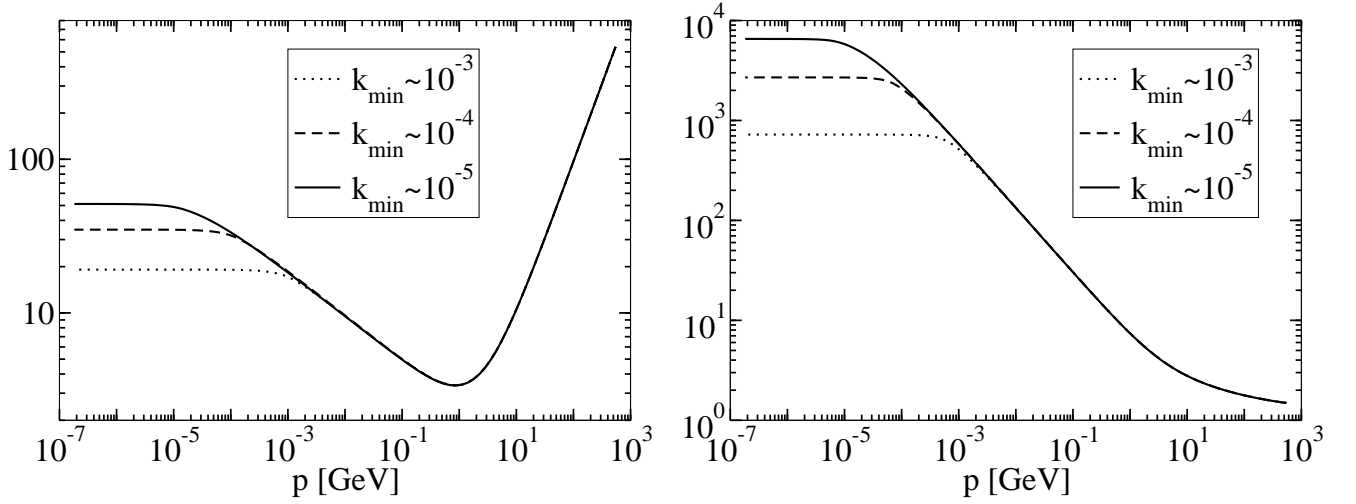


FIG. 6: Gluon propagator ω (left) and ghost dressing d (right) for different minimal cutoffs k_{min}

$$\partial_t \omega_k(p) = -\frac{N_c}{2} \int \frac{d^3 q}{(2\pi)^3} \left(\bar{G}_{c,k} \dot{R}_{c,k} \bar{G}_{c,k} \right) (q) \bar{G}_{c,k}(|\mathbf{p} + \mathbf{q}|) q^2 (1 - (\hat{\mathbf{p}} \cdot \hat{\mathbf{q}})^2), \quad (53)$$

$$\begin{aligned} \partial_t d_k^{-1}(p) = N_c p^2 \int \frac{d^3 q}{(2\pi)^3} & \left[\left(G_{A,k} \dot{R}_{A,k} G_{A,k} \right) (q) \bar{G}_{c,k}(|\mathbf{p} + \mathbf{q}|) \right. \\ & \left. + \left(\bar{G}_{c,k} \dot{R}_{c,k} \bar{G}_{c,k} \right) (q) G_{A,k}(|\mathbf{p} + \mathbf{q}|) \frac{q^2}{(\mathbf{p} + \mathbf{q})^2} \right] (1 - (\hat{\mathbf{p}} \cdot \hat{\mathbf{q}})^2). \end{aligned} \quad (54)$$

The computation is detailed in Appendix C. Eqs. (53) and (54) are two coupled functional ordinary differential equations for ω_k and d_k , which can be solved numerically. Due to our definition (48) of the ghost form factor $d_k(p)$ the bare coupling constant g has formally disappeared from the propagator flow equations. Let us stress again that a physically meaningful renormalization group invariant coupling is defined by Eq. (52). To incorporate the appropriate initial conditions it is convenient to cast the differential flow equations into an integral form,

$$\omega_k(p) - \omega_\Lambda(p) = \int_\Lambda^k \frac{dk'}{k'} \int \frac{d^3 \ell}{(2\pi)^3} I_{k'}^\omega[d_{k'}](\ell, \mathbf{p}), \quad (55)$$

$$d_k^{-1}(p) - d_\Lambda^{-1}(p) = \int_\Lambda^k \frac{dk'}{k'} \int \frac{d^3 \ell}{(2\pi)^3} I_{k'}^d[\omega_{k'}, d_{k'}](\ell, \mathbf{p}). \quad (56)$$

I^ω and I^d stand for the integrands of the loop integrals on the r.h.s. of Eqs. (53) and (54).

The initial conditions $d_\Lambda(p), \omega_\Lambda(p)$ for the flow can be determined by perturbation theory [27, 31]. Due to the kinematic structure of the ghost-gluon vertex no mass term for the ghost is produced. Moreover, contributions

with higher powers of momenta than the ones in lowest-order perturbation theory, $d^{(0)}(p) = 1$ and $\omega^{(0)}(p) = p$, are suppressed by the corresponding powers of Λ . Note, however, that there is additional logarithmic scaling. In the case of $d_\Lambda(p)$, this implies that for a large initial cut-off scale $k = \Lambda$ we only have to fix the constant $d_\Lambda(p) \equiv d_\Lambda$.

For the gluon the introduction of the regulator term enforces a mass-like term, i.e., a p -independent contribution to $\omega_k(p)$, due to the modified Slavnov-Taylor identities (mSTI), see e.g. [1, 8, 10, 33, 34]. We rush to add that the direct use of the mSTI in the infrared is not advisable as the mSTI only fix the longitudinal mass which does not relate to the transverse one in the infrared [1, 8, 35]. We conclude that for large initial cut-off scales $k = \Lambda$ the inverse gluon propagator has two relevant parameters, the mass-like parameter a and the coefficient of the classical term. The latter is put to one and we have $\omega_\Lambda(p) = p + a$.

It is evident from the form of the flow equations in (55), (56) that the solution will not show infrared scaling unless the parameter $d_\Lambda^{-1}(p) \equiv d_\Lambda^{-1}$ is fine-tuned (at least for $\beta = 2\kappa_c > 0$). Such fine-tuning of relevant parameters is a well-known initial condition problem for RG flows. Indeed, it also occurs in Landau gauge Yang-Mills the-

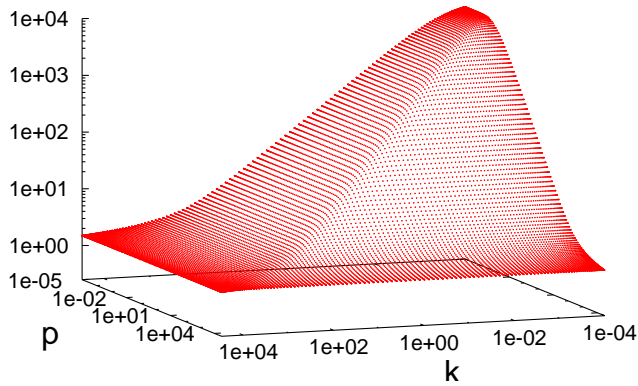


FIG. 7: The flow of the full ghost form factor, $d_k(p)$, is shown. The gradual formation of the IR power law when lowering the cutoff scale k is explicitly seen.

ory, see e.g. [1, 35, 36], where it is directly related to the resolution of the Gribov problem, see [1, 4]. In [1] it has also been shown that there is a full one parameter family of solutions compatible with non-perturbative renormalization where only the endpoint shows a scaling behavior whereas the other solutions show a decoupling behavior: a gluon with a mass-like propagator and a ghost which is at most logarithmically enhanced. Such a scenario very likely also applies to Coulomb gauge and hence deserves further investigation.

In the present case we have numerically solved the fine-tuning condition for d_Λ with the constraint of infrared scaling for the ghost dressing function. The parameter a in the initial condition $\omega_\Lambda(p)$ is fixed by demanding that $\omega(p)$ reduce to the perturbative form $\omega(p) \propto p$ for “large” momenta p close to but below Λ . The regulator used in the numerical solution is

$$r_k(p) = \exp\left(\frac{k^2}{p^2} - \frac{p^2}{k^2}\right). \quad (57)$$

Our numerical procedure is detailed in Appendix D. The results for the inverse gluon propagator $\omega_k(p)$ and the ghost dressing function $d_k(p)$ are shown in Fig. 6 for different values of the minimal cutoff k_{min} down to which the flow integration has been carried out. It is seen that the power law behavior in both cases extends towards the IR as the cutoff k_{min} is lowered, although we have implemented a scaling behavior - not the “horizon condition” $d_0^{-1}(p=0) = 0$ - only for the ghost dressing. Thus, we arrive at the nontrivial result that a solution for the flow equations can be found that obeys a power law behavior (43) for both the gluon and the ghost propagator. For the sake of illustration, we also display the full flow of the ghost dressing function, $d_k(p)$, in Fig. 7.

The IR power laws are extracted from the numerical solution shown in Fig. 6. The scaling coefficients α, β defined in (43) are computed as

$$\omega(p \rightarrow 0) \sim p^{-\alpha}, \quad d(p \rightarrow 0) \sim p^{-\beta}. \quad (58)$$

and with the numerical solution we get

$$\alpha = 0.28, \quad \beta = 0.64, \quad (59)$$

and hence α and β satisfy the sum rule (44), already found for the Coulomb gauge DSE in [17]. Note however that the scaling coefficients obtained in the present truncation differ from the ones obtained in the DSE. In Fig. 8 the solutions of the FRG flow equation for $\omega(p)$ and $d(p)$ are compared to the results obtained from an optimized calculation in sect. IV C which in turn are precisely the results found in [15] by a variational calculation, see Fig. 9. This variational calculation gave rise to the DSEs which will be found in sect. IV C as approximation to the full flow equation. While the curves in Fig. 8 match in the UV, the results of the FRG in the present minimal truncation are less infrared enhanced than the ones of the DSE. Note that the scaling coefficients are expected to depend on the chosen regulator. It has been already proven in [36] for Landau gauge Yang-Mills theory that the scaling coefficients of FRG and DSE agree for optimized regulators if a bare ghost-gluon vertex is used. Optimized regulators are those that maximize the physics content of a given truncation scheme at a given order, for details of the optimization theory for the FRG we refer the reader to [8, 37]. The details of the arguments put forward in [36] directly carry over to the Coulomb gauge system.

C. Optimization

In this chapter we shall use the optimization arguments hinted at above in order to optimize the physics content of our present truncation. Similar, but more refined arguments have been used in Landau gauge for arriving at FRG results for the propagators that quantitatively agree with the lattice results [1, 35], the details will be published in [35]. Here we first follow the arguments put forward in [36]. To that end consider the following approximation: under the loop integrals we replace the propagators at the running momentum scale k, ω_k and d_k , by the propagators of the full theory, i.e. the ones at zero scale $k = 0$:

$$d_k(p) \rightarrow d_{k=0}(p), \quad \omega_k(p) \rightarrow \omega_{k=0}(p). \quad (60)$$

Note that this does only imply that the difference between the propagators at $k = 0$ and the regularized ones at k drops out in the integrals. Indeed one can explicitly construct regulators for which this holds true in the asymptotic IR region, see [36]. Note that due to the strong infrared suppression introduced with the regulator choice (57) the approximation (60) is quantitatively reliable inside the loop integrals except for a small range of momenta p around the scale k . The approximation (60) allows us to analytically integrate the flow equations (53), (54) over k . The only k -dependence left is the explicit one on the regulator as the vertices are not k -dependent

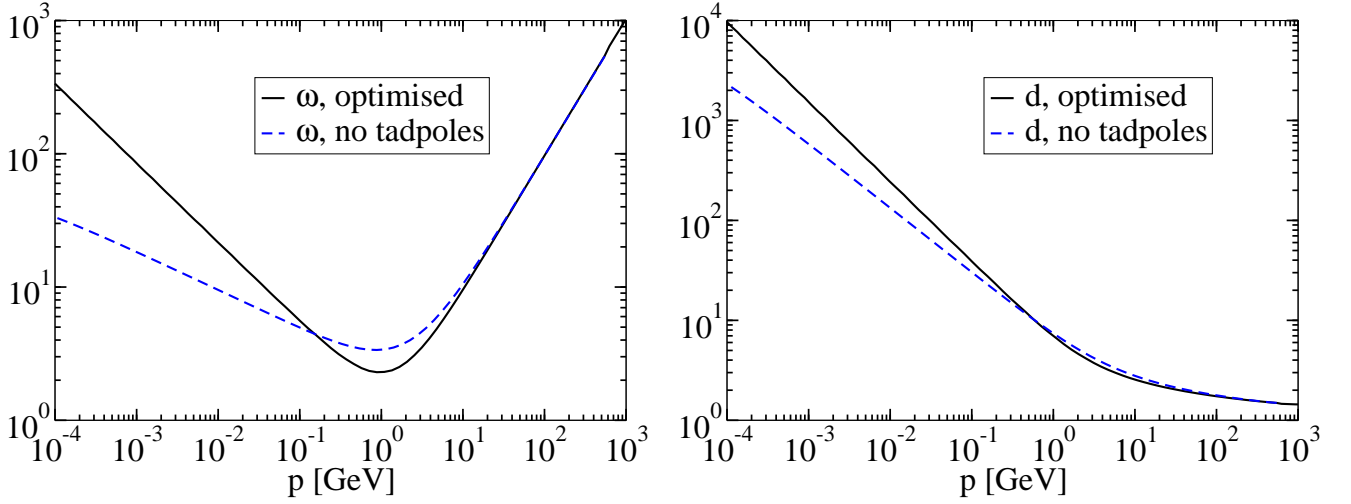


FIG. 8: Comparison of the gluon propagators ω (left) and the ghost dressings d (right) calculated from the optimized flow and from the flow without tadpoles.

from the outset. Hence the flow can be rewritten as a total t -derivative of the loop integrals with full propagators

and we arrive at

$$(d_0^{-1} - d_\Lambda^{-1})(p) = -N_c \int \frac{d^3 q}{(2\pi)^3} \frac{1}{2\omega_0(q) + R_{A,k}(q)} \frac{(1 - (\hat{\mathbf{p}} \cdot \hat{\mathbf{q}})^2)}{(\mathbf{p} + \mathbf{q})^2 d_0^{-1}(|\mathbf{p} + \mathbf{q}|) + \bar{R}_{c,k}(|\mathbf{p} + \mathbf{q}|)} \Big|_{k=\Lambda}^{k=0}, \quad (61)$$

$$(\omega_0 - \omega_\Lambda)(p) = \frac{N_c}{4} \int \frac{d^3 q}{(2\pi)^3} \frac{q^2}{q^2 d_0^{-1}(q) + \bar{R}_{c,k}(q)} \frac{(1 - (\hat{\mathbf{p}} \cdot \hat{\mathbf{q}})^2)}{(\mathbf{p} + \mathbf{q})^2 d_0^{-1}(|\mathbf{p} + \mathbf{q}|) + \bar{R}_{c,k}(|\mathbf{p} + \mathbf{q}|)} \Big|_{k=\Lambda}^{k=0}. \quad (62)$$

We notice that the flow equations (61), (62) have acquired the form of DSEs. Given the fact that $R_{k=0} = 0$ (see Eq. (3)) these equations coincide with the DSEs obtained in [15] (to be precise, the DSE for $\omega(p)$ in [15] contains additional contributions which are, however, subleading in the infrared), with a different UV-regularization realized here through the $(k = \Lambda)$ -terms. Moreover, the optimization arguments in [8, 36] imply that the flows (61), (62) provide the best approximation to the full theory for the IR asymptotics. In [35] it is shown that in the given truncation this argument extends to the full momentum regime: by adding the tadpole diagrams related to ghost-only and ghost-gluon vertices to the flow equations displayed in Figs. 4, 5 and using the DSE for the tadpole vertices in the flows one can show that this leads to the integrated flow (61), (62). If we also add the gluonic diagrams, this argument gets more involved.

It remains to adjust the initial conditions. We could proceed in the same way as for the numerical solution in the last subsection to implement the condition of infrared scaling for the ghost dressing function. However,

it is much simpler to use as an input the information from this numerical solution that $\beta = 2\kappa > 0$ and thus $d_0^{-1}(p = 0) = 0$ (the horizon condition), so we can write

$$d_0^{-1}(p) = \int \frac{d^3 q}{(2\pi)^3} [\text{int}(k, \mathbf{p}, \mathbf{q}) - \text{int}(k, \mathbf{p} = 0, \mathbf{q})] \Big|_{k=\Lambda}^{k=0}, \quad (63)$$

where $\text{int}(k, \mathbf{p}, \mathbf{q})$ denotes the integrand in (61). More details of the numerical procedure can be found in Appendix D.

The results of the iteration are shown in Fig. 9. A power law as in Eq. (58) emerges in the infrared region for both the gluon energy $\omega(p)$ and the ghost dressing function $d(p)$ with the IR exponents

$$\alpha = 0.60, \quad \beta = 0.80, \quad (64)$$

which is precisely one of the two possible IR solutions found analytically for the DSE in [17]. Furthermore, it corresponds to the solution found in the variational approach [15]. It must be noted that the second possible solution in the analytical approach of Ref. [17] has also been confirmed in a numerical variational calculation

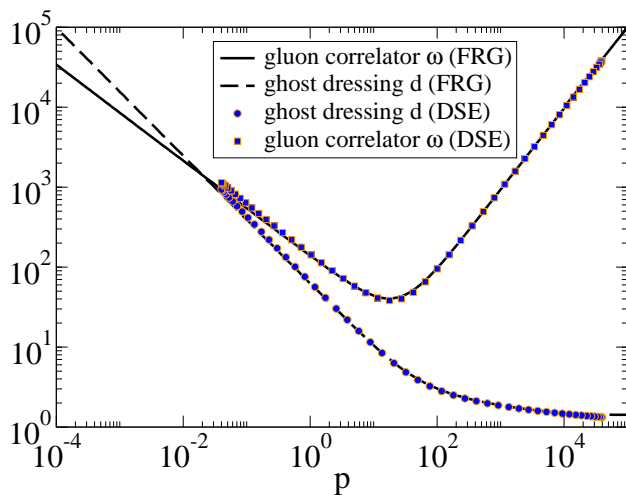


FIG. 9: Gluon propagator ω and ghost dressing function d from the optimized flow equation in comparison with the results of the DSEs obtained from the variational ansatz in [15]. The results lie on top of each other as expected.

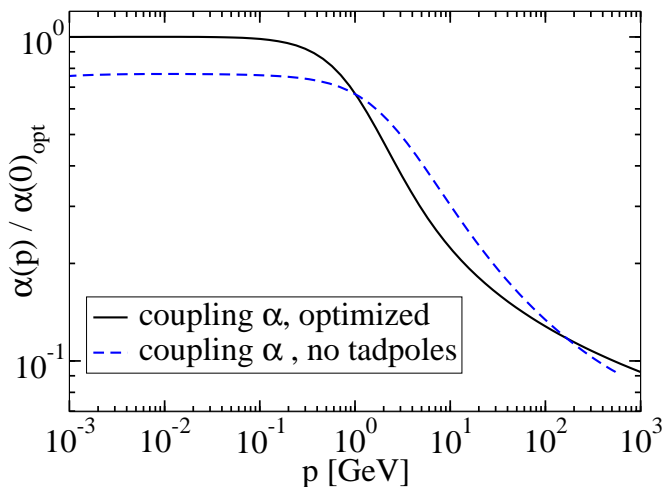


FIG. 10: The running coupling constant $\alpha = g_R^2/4\pi$, Eq. (52), calculated from the optimized flow and from the flow without tadpoles.

[18]. Indeed, it is also present in our optimized approximation which has the identical infrared properties as the DSE. However, it is not clear to us at present whether after the inclusion of the gluonic diagrams this solution persists as an infrared stable one. Note in this context that it requires additional fine-tuning and hence may be unstable.

Finally, in Fig. 10, we show the running coupling constant $\alpha = g_R^2/4\pi$, see Eq. (52), calculated by using the propagators from the optimized flow equation as well as from the flow equation without the tadpoles. The plateau in the IR is due to the sum rule (44) which is fulfilled by the propagators resulting from both approximations of the flow equations.

V. CONCLUSIONS

We have presented a new approach to the non-perturbative calculation of static propagators, or correlation functions at equal times, from the Hamiltonian formulation of a quantum field theory. In the generating functional of the correlation functions at equal times, (minus twice) the logarithm of the modulus of the vacuum wave functional comes to play the role of the Euclidean action in the usual covariant theory. We have then adapted the functional renormalization group to this Hamiltonian formulation.

This new approach has subsequently been applied to Yang-Mills theory in the Coulomb gauge. The derivation of the corresponding flow equations for the propagators has been presented in detail. In order to arrive at a closed system of equations, we have replaced the dressed ghost-gluon vertex with the corresponding bare one (or a vertex with constant dressing, a good approximation according to perturbative arguments and lattice calculations), and we have neglected all tadpole diagrams and vertices with three or more gluon lines. We have also presented an approximation that allows for an analytical integration of the flow equations and have argued that it actually corresponds to an optimized choice of the regulator functions. We have discussed in detail the choice of the initial conditions which serve to implement the normalization conditions corresponding to an infrared scaling solution for the propagators.

The result of the numerical solution of the flow equations has been compared to the solution of a system of Dyson-Schwinger equations derived from a variational principle for the vacuum wave functional. The solution of the flow equations agrees with one of the two possible scaling solutions in the latter approach. In the approximation without tadpoles we have obtained slightly different values for the infrared anomalous dimensions than from the Dyson-Schwinger equations. Indeed, in this truncation the anomalous dimensions mildly depend on the regulator functions and only agree with the Dyson-Schwinger values for optimized regulators, as has been argued in [36]. In the optimized approximation the infrared anomalous dimensions are regulator-independent. This supports the reliability of the optimized approximation.

We have not presented the second scaling solution which poses an additional fine-tuning problem. Its resolution also allows to study the interesting question of infrared stability of this solution, and will be discussed elsewhere.

Note also that the formalism put forward in the present work allows to directly access the confining properties of the propagators. This can be done by using the Wilson loop potential evaluated in [38]. Moreover one can study full dynamical QCD in Coulomb gauge along the lines of [39]. A first step in this direction is to implement the missing gluonic diagrams for a comparison with lattice data in the full momentum regime. These investigations

will certainly shed more light on the pressing unresolved questions of low energy QCD.

Acknowledgments

M.L. was supported by the Internationales Graduiertenkolleg “Hadronen im Vakuum, in Kernen und Sternen”. J.M.P. acknowledges support by Helmholtz Alliance HA216/EMMI. H.R. acknowledges support by DFG-Re856/6-3. A.W. would like to thank the Deutscher Akademischer Austauschdienst (DAAD), Conacyt project no. 46513-F, and CIC-UMSNH for financial support.

Appendix A: Details of the derivation of the flow of the effective action

In this appendix we fill in some of the details of the derivation of the flow equation (39). From the regularized generating functional (25) and Eq. (27), we derive the flow equation

$$\partial_t Z_k[J, \sigma, \bar{\sigma}] = \left(-\frac{1}{2} \frac{\delta}{\delta J} \cdot \dot{R}_{A,k} \cdot \frac{\delta}{\delta J} + \frac{\delta}{\delta \sigma} \cdot \dot{R}_{c,k} \cdot \frac{\delta}{\delta \sigma}\right) Z_k[J, \sigma, \bar{\sigma}], \quad (\text{A1})$$

where the difference in signs of the gluon and ghost regulator term compared to Eq. (27) is due to the Grassmann property of the ghost fields and sources.

The definition of the Schwinger functional W_k generating connected Green functions reads

$$W_k[J, \sigma, \bar{\sigma}] := \ln Z_k[J, \sigma, \bar{\sigma}], \quad (\text{A2})$$

and therefore its flow is

$$\begin{aligned} \partial_t W_k = & \left(-\frac{1}{2} \frac{\delta W_k}{\delta J} \cdot \dot{R}_{A,k} \cdot \frac{\delta W_k}{\delta J} - \frac{1}{2} \text{Tr} \dot{R}_{A,k} \frac{\delta^2 W_k}{\delta J \delta J} \right. \\ & \left. + \frac{\delta W_k}{\delta \sigma} \cdot \dot{R}_{c,k} \cdot \frac{\delta W_k}{\delta \sigma} - \text{Tr} \dot{R}_{c,k} \frac{\delta^2 W_k}{\delta \sigma \delta \sigma} \right). \end{aligned} \quad (\text{A3})$$

The effective action Γ_k is defined via a modified Legendre transformation,

$$\begin{aligned} \Gamma_k[A, \bar{c}, c] := & -W_k[J_k, \sigma_k, \bar{\sigma}_k] + J_k \cdot A + \bar{\sigma}_k \cdot c + \bar{c} \cdot \sigma_k \\ & - \frac{1}{2} A \cdot R_{A,k} \cdot A - \bar{c} \cdot R_{c,k} \cdot c, \end{aligned} \quad (\text{A4})$$

which turns into the usual one upon taking $k \rightarrow 0$, because $R_{A,k=0} = R_{c,k=0} = 0$. In Eq. (A4), the sources are functionals of the fields (whose notation is suppressed), which are the expectation values of the corresponding field operators. The relations between sources and fields are given by

$$\begin{aligned} A_i^a(-\mathbf{p}) &= (2\pi)^3 \frac{\delta W_k[J_k, \sigma_k, \bar{\sigma}_k]}{\delta J_i^a(\mathbf{p})}, \\ c^a(-\mathbf{p}) &= (2\pi)^3 \frac{\delta W_k[J_k, \sigma_k, \bar{\sigma}_k]}{\delta \bar{\sigma}^a(\mathbf{p})}, \\ \bar{c}^a(-\mathbf{p}) &= - (2\pi)^3 \frac{\delta W_k[J_k, \sigma_k, \bar{\sigma}_k]}{\delta \sigma^a(\mathbf{p})}, \end{aligned} \quad (\text{A5})$$

or shorthand

$$A^a = \frac{\delta W_k}{\delta J^a}, \quad c = \frac{\delta W_k}{\delta \bar{\sigma}}, \quad \bar{c} = -\frac{\delta W_k}{\delta \sigma}. \quad (\text{A6})$$

With these definitions and with Eq. (A3), the flow of the effective action is written as

$$\begin{aligned} \partial_t \Gamma_k = & -(\partial_t W_k)[J_k, \sigma_k, \bar{\sigma}_k] \\ & - \partial_t J_k \cdot \frac{\delta W_k}{\delta J} - \partial_t \sigma_k \cdot \frac{\delta W_k}{\delta \sigma} - \partial_t \bar{\sigma}_k \cdot \frac{\delta W_k}{\delta \bar{\sigma}} \\ & + A \cdot \partial_t J_k + \partial_t \bar{\sigma}_k \cdot c - \partial_t \sigma_k \cdot \bar{c} \\ & - \frac{1}{2} A \cdot \dot{R}_{A,k} \cdot A - \bar{c} \cdot \dot{R}_{c,k} \cdot c \\ = & \left(\frac{1}{2} \text{Tr} \dot{R}_{A,k} \frac{\delta^2 W_k}{\delta J \delta J} + \text{Tr} \dot{R}_{c,k} \frac{\delta^2 W_k}{\delta \bar{\sigma} \delta \sigma} \right) \Big|_{J_k, \sigma_k, \bar{\sigma}_k}. \end{aligned} \quad (\text{A7})$$

When expressed in the superfield notation introduced from Eq. (31) on, this equation turns into Eq. (37) and finally into Eq. (39). In components of the superfield, Eq. (39) reads

$$\partial_t \Gamma_k = \frac{1}{2} \text{Tr} \begin{pmatrix} \dot{R}_{A,k} & & \\ & -\dot{R}_{c,k} & \\ & & -\dot{R}_{c,k}^T \end{pmatrix} \begin{pmatrix} \frac{\delta^2 \Gamma_k}{\delta A \delta A} + R_{A,k} & \frac{\delta^2 \Gamma_k}{\delta A \delta c} & \frac{\delta^2 \Gamma_k}{\delta A \delta \bar{c}} \\ -\frac{\delta^2 \Gamma_k}{\delta \bar{c} \delta A} & -\frac{\delta^2 \Gamma_k}{\delta \bar{c} \delta c} + R_{c,k} & -\frac{\delta^2 \Gamma_k}{\delta \bar{c} \delta \bar{c}} \\ \frac{\delta^2 \Gamma_k}{\delta c \delta A} & \frac{\delta^2 \Gamma_k}{\delta c \delta c} & \frac{\delta^2 \Gamma_k}{\delta c \delta \bar{c}} + R_{c,k}^T \end{pmatrix}^{-1}. \quad (\text{A8})$$

From this equation we derive the flow equations for the ghost and gluon fields by taking functional derivatives w.r.t. these fields.

Appendix B: Details of the derivation of the propagator flows

In this section we derive the flow equations for the propagators from the flow equation for the effective action, Eq. (A8). A useful relation for the following concerns the commutation of fermionic derivatives past supermatrices. Consider a matrix with a block structure of commuting (c) and anticommuting (a) quantities and an

anticommuting η :

$$\eta \begin{pmatrix} c & a & a \\ a & c & c \\ a & c & c \end{pmatrix} = \begin{pmatrix} c & -a & -a \\ -a & c & c \\ -a & c & c \end{pmatrix} \eta = M \begin{pmatrix} c & a & a \\ a & c & c \\ a & c & c \end{pmatrix} M \eta. \quad (\text{B1})$$

This matrix structure is shared by $\delta^2 \Gamma_k / \delta \bar{\phi} \delta \phi$ as well as $(\delta^2 \Gamma_k / \delta \bar{\phi} \delta \phi + \mathcal{R}_k)^{-1}$, the latter because of Eq. (38).

In the following, i and j are condensed external indices. They stand for color indices, momenta and, in the case of gluon fields, also vector indices at the same time. They are, however, not part of the matrix notation. From

$$\begin{aligned} 0 &= \frac{\delta}{\delta c_i} \left(\left(\frac{\delta^2 \Gamma_k}{\delta \bar{\phi} \delta \phi} + \mathcal{R}_k \right) \left(\frac{\delta^2 \Gamma_k}{\delta \bar{\phi} \delta \phi} + \mathcal{R}_k \right)^{-1} \right) \\ &= \frac{\delta^3 \Gamma_k}{\delta c_i \delta \bar{\phi} \delta \phi} \left(\frac{\delta^2 \Gamma_k}{\delta \bar{\phi} \delta \phi} + \mathcal{R}_k \right)^{-1} + M \left(\frac{\delta^2 \Gamma_k}{\delta \bar{\phi} \delta \phi} + \mathcal{R}_k \right) M \frac{\delta}{\delta c_i} \left(\frac{\delta^2 \Gamma_k}{\delta \bar{\phi} \delta \phi} + \mathcal{R}_k \right)^{-1} \end{aligned} \quad (\text{B2})$$

it follows that

$$\frac{\delta}{\delta c_i} \left(\frac{\delta^2 \Gamma_k}{\delta \bar{\phi} \delta \phi} + \mathcal{R}_k \right)^{-1} = -M \left(\frac{\delta^2 \Gamma_k}{\delta \bar{\phi} \delta \phi} + \mathcal{R}_k \right)^{-1} M \frac{\delta^3 \Gamma_k}{\delta c_i \delta \bar{\phi} \delta \phi} \left(\frac{\delta^2 \Gamma_k}{\delta \bar{\phi} \delta \phi} + \mathcal{R}_k \right)^{-1}. \quad (\text{B3})$$

For bosonic derivatives the same formula holds without the M 's. Using this, we can derive the ghost propagator flow equation from the flow of the effective action, Eq. (A8):

$$\begin{aligned} \frac{\delta^2 \dot{\Gamma}_k}{\delta \bar{c}_j \delta c_i} &= \frac{1}{2} \frac{\delta^2}{\delta \bar{c}_j \delta c_i} \text{STr} \left[\dot{\mathcal{R}}_k \left(\frac{\delta^2 \Gamma_k}{\delta \bar{\phi} \delta \phi} + \mathcal{R}_k \right)^{-1} \right] \\ &= \frac{1}{2} \frac{\delta}{\delta \bar{c}_j} \text{STr} \left[-\dot{\mathcal{R}}_k M \left(\frac{\delta^2 \Gamma_k}{\delta \bar{\phi} \delta \phi} + \mathcal{R}_k \right)^{-1} M \frac{\delta^3 \Gamma_k}{\delta c_i \delta \bar{\phi} \delta \phi} \left(\frac{\delta^2 \Gamma_k}{\delta \bar{\phi} \delta \phi} + \mathcal{R}_k \right)^{-1} \right] \\ &= \frac{1}{2} \text{STr} \left[\dot{\mathcal{R}}_k \left(\frac{\delta^2 \Gamma_k}{\delta \bar{\phi} \delta \phi} + \mathcal{R}_k \right)^{-1} M \frac{\delta^3 \Gamma_k}{\delta \bar{c}_j \delta \bar{\phi} \delta \phi} \left(\frac{\delta^2 \Gamma_k}{\delta \bar{\phi} \delta \phi} + \mathcal{R}_k \right)^{-1} M \frac{\delta^3 \Gamma_k}{\delta c_i \delta \bar{\phi} \delta \phi} \left(\frac{\delta^2 \Gamma_k}{\delta \bar{\phi} \delta \phi} + \mathcal{R}_k \right)^{-1} \right] \\ &\quad - \frac{1}{2} \text{STr} \left[\dot{\mathcal{R}}_k \left(\frac{\delta^2 \Gamma_k}{\delta \bar{\phi} \delta \phi} + \mathcal{R}_k \right)^{-1} M \frac{\delta^3 \Gamma_k}{\delta c_i \delta \bar{\phi} \delta \phi} \left(\frac{\delta^2 \Gamma_k}{\delta \bar{\phi} \delta \phi} + \mathcal{R}_k \right)^{-1} M \frac{\delta^3 \Gamma_k}{\delta \bar{c}_j \delta \bar{\phi} \delta \phi} \left(\frac{\delta^2 \Gamma_k}{\delta \bar{\phi} \delta \phi} + \mathcal{R}_k \right)^{-1} \right] \\ &\quad - \frac{1}{2} \text{STr} \left[\dot{\mathcal{R}}_k \left(\frac{\delta^2 \Gamma_k}{\delta \bar{\phi} \delta \phi} + \mathcal{R}_k \right)^{-1} \frac{\delta^4 \Gamma_k}{\delta \bar{c}_j \delta c_i \delta \bar{\phi} \delta \phi} \left(\frac{\delta^2 \Gamma_k}{\delta \bar{\phi} \delta \phi} + \mathcal{R}_k \right)^{-1} \right]. \end{aligned} \quad (\text{B4})$$

Setting the fields to zero, $A = \bar{c} = c = 0$, only the block matrices with the same number of ghosts and antighosts remain. With the definition

$$\mathcal{G}_k := \begin{pmatrix} \left(\frac{\delta^2 \Gamma_k}{\delta A \delta A} + R_{A,k} \right)^{-1} & 0 & 0 \\ 0 & \left(-\frac{\delta^2 \Gamma_k}{\delta \bar{c} \delta c} + R_{c,k} \right)^{-1} & 0 \\ 0 & 0 & \left(\frac{\delta^2 \Gamma_k}{\delta c \delta \bar{c}} + R_{c,k}^T \right)^{-1} \end{pmatrix} \quad (\text{B5})$$

the first of the three terms in Eq. (B4) becomes

$$\frac{1}{2} \text{Tr} \begin{pmatrix} \dot{R}_{A,k} & 0 & 0 \\ 0 & -\dot{R}_{c,k} & 0 \\ 0 & 0 & -\dot{R}_{c,k}^T \end{pmatrix} \mathcal{G}_k \begin{pmatrix} 0 & \frac{\delta^3 \Gamma_k}{\delta \bar{c}_j \delta A \delta c} & 0 \\ 0 & 0 & 0 \\ -\frac{\delta^3 \Gamma_k}{\delta \bar{c}_j \delta c \delta A} & 0 & 0 \end{pmatrix} \mathcal{G}_k \begin{pmatrix} 0 & 0 & \frac{\delta^3 \Gamma_k}{\delta c_i \delta A \delta \bar{c}} \\ \frac{\delta^3 \Gamma_k}{\delta c_i \delta \bar{c} \delta A} & 0 & 0 \\ 0 & 0 & 0 \end{pmatrix} \mathcal{G}_k \quad (\text{B6})$$

$$\begin{aligned} &= \frac{1}{2} \text{Tr} \dot{R}_{A,k} \left(\frac{\delta^2 \Gamma_k}{\delta A \delta A} + R_{A,k} \right)^{-1} \frac{\delta^3 \Gamma_k}{\delta \bar{c}_j \delta A \delta c} \left(-\frac{\delta^2 \Gamma_k}{\delta \bar{c} \delta c} + R_{c,k} \right)^{-1} \frac{\delta^3 \Gamma_k}{\delta c_i \delta \bar{c} \delta A} \left(\frac{\delta^2 \Gamma_k}{\delta A \delta A} + R_{A,k} \right)^{-1} \\ &+ \frac{1}{2} \text{Tr} \dot{R}_{c,k}^T \left(\frac{\delta^2 \Gamma_k}{\delta c \delta \bar{c}} + R_{c,k}^T \right)^{-1} \frac{\delta^3 \Gamma_k}{\delta \bar{c}_j \delta c \delta A} \left(\frac{\delta^2 \Gamma_k}{\delta A \delta A} + R_{A,k} \right)^{-1} \frac{\delta^3 \Gamma_k}{\delta c_i \delta A \delta \bar{c}} \left(\frac{\delta^2 \Gamma_k}{\delta c \delta \bar{c}} + R_{c,k}^T \right)^{-1}. \end{aligned} \quad (\text{B7})$$

The other two terms are treated alike. The ghost flow equation then reads (using $R_{c,k}^T = R_{c,k}$)

$$\begin{aligned} \frac{\delta^2 \dot{\Gamma}_k}{\delta \bar{c}_j \delta c_i} &= \text{Tr} \dot{R}_{A,k} \left(\frac{\delta^2 \Gamma_k}{\delta A \delta A} + R_{A,k} \right)^{-1} \frac{\delta^3 \Gamma_k}{\delta \bar{c}_j \delta A \delta c} \left(-\frac{\delta^2 \Gamma_k}{\delta \bar{c} \delta c} + R_{c,k} \right)^{-1} \frac{\delta^3 \Gamma_k}{\delta c_i \delta \bar{c} \delta A} \left(\frac{\delta^2 \Gamma_k}{\delta A \delta A} + R_{A,k} \right)^{-1} \\ &+ \text{Tr} \dot{R}_{c,k} \left(-\frac{\delta^2 \Gamma_k}{\delta \bar{c} \delta c} + R_{c,k} \right)^{-1} \frac{\delta^3 \Gamma_k}{\delta c_i \delta \bar{c} \delta A} \left(\frac{\delta^2 \Gamma_k}{\delta A \delta A} + R_{A,k} \right)^{-1} \frac{\delta^3 \Gamma_k}{\delta \bar{c}_j \delta A \delta c} \left(-\frac{\delta^2 \Gamma_k}{\delta \bar{c} \delta c} + R_{c,k} \right)^{-1} \\ &- \frac{1}{2} \text{Tr} \dot{R}_{A,k} \left(\frac{\delta^2 \Gamma_k}{\delta A \delta A} + R_{A,k} \right)^{-1} \frac{\delta^4 \Gamma_k}{\delta \bar{c}_j \delta c_i \delta A \delta A} \left(\frac{\delta^2 \Gamma_k}{\delta A \delta A} + R_{A,k} \right)^{-1} \\ &- \text{Tr} \dot{R}_{c,k} \left(-\frac{\delta^2 \Gamma_k}{\delta \bar{c} \delta c} + R_{c,k} \right)^{-1} \frac{\delta^4 \Gamma_k}{\delta \bar{c}_j \delta c_i \delta \bar{c} \delta c} \left(-\frac{\delta^2 \Gamma_k}{\delta \bar{c} \delta c} + R_{c,k} \right)^{-1}. \end{aligned} \quad (\text{B8})$$

In much the same way, the gluon flow equation is deduced from Eq. (A8), and the result is

$$\begin{aligned} \frac{\delta^2 \dot{\Gamma}_k}{\delta A_j \delta A_i} &= \text{Tr} \dot{R}_{A,k} \left(\frac{\delta^2 \Gamma_k}{\delta A \delta A} + R_{A,k} \right)^{-1} \frac{\delta^3 \Gamma_k}{\delta A_j \delta A \delta A} \left(\frac{\delta^2 \Gamma_k}{\delta A \delta A} + R_{A,k} \right)^{-1} \frac{\delta^3 \Gamma_k}{\delta A_i \delta A \delta A} \left(\frac{\delta^2 \Gamma_k}{\delta A \delta A} + R_{A,k} \right)^{-1} \\ &- \text{Tr} \dot{R}_{c,k} \left(-\frac{\delta^2 \Gamma_k}{\delta \bar{c} \delta c} + R_{c,k} \right)^{-1} \frac{\delta^3 \Gamma_k}{\delta A_j \delta \bar{c} \delta c} \left(-\frac{\delta^2 \Gamma_k}{\delta \bar{c} \delta c} + R_{c,k} \right)^{-1} \frac{\delta^3 \Gamma_k}{\delta A_i \delta \bar{c} \delta c} \left(-\frac{\delta^2 \Gamma_k}{\delta \bar{c} \delta c} + R_{c,k} \right)^{-1} \\ &- \text{Tr} \dot{R}_{c,k} \left(-\frac{\delta^2 \Gamma_k}{\delta \bar{c} \delta c} + R_{c,k} \right)^{-1} \frac{\delta^3 \Gamma_k}{\delta A_i \delta \bar{c} \delta c} \left(-\frac{\delta^2 \Gamma_k}{\delta \bar{c} \delta c} + R_{c,k} \right)^{-1} \frac{\delta^3 \Gamma_k}{\delta A_j \delta \bar{c} \delta c} \left(-\frac{\delta^2 \Gamma_k}{\delta \bar{c} \delta c} + R_{c,k} \right)^{-1} \\ &- \frac{1}{2} \text{Tr} \dot{R}_{A,k} \left(\frac{\delta^2 \Gamma_k}{\delta A \delta A} + R_{A,k} \right)^{-1} \frac{\delta^4 \Gamma_k}{\delta A_j \delta A_i \delta A \delta A} \left(\frac{\delta^2 \Gamma_k}{\delta A \delta A} + R_{A,k} \right)^{-1} \\ &- \text{Tr} \dot{R}_{c,k} \left(-\frac{\delta^2 \Gamma_k}{\delta \bar{c} \delta c} + R_{c,k} \right)^{-1} \frac{\delta^4 \Gamma_k}{\delta A_j \delta A_i \delta \bar{c} \delta c} \left(-\frac{\delta^2 \Gamma_k}{\delta \bar{c} \delta c} + R_{c,k} \right)^{-1}. \end{aligned} \quad (\text{B9})$$

These equations are represented diagrammatically in Figs. 2, 3.

Appendix C: Explicit form of the flow equations

In this appendix we will use the parametrization of sect. IV A in order to bring the truncated flow equations represented in Figs. 4, 5 into their final form.

As the ghost two-point function and the ghost regulator are both diagonal in color space and momentum space, they can easily be inverted, yielding (see Eqs. (29), (48), (49), (50))

$$\begin{aligned} \left[\left(-\frac{\delta^2 \Gamma_k}{\delta \bar{c} \delta c} + R_{c,k} \right)^{-1} \right]_{\mathbf{p}\mathbf{q}}^{ab} &= \delta^{ab} [g p^2 / d_k(p) + R_{c,k}(p)]^{-1} (2\pi)^3 \delta^3(\mathbf{p} + \mathbf{q}) \\ &= \delta^{ab} \frac{1}{g} \bar{G}_{c,k}(p) (2\pi)^3 \delta^3(\mathbf{p} + \mathbf{q}) . \end{aligned} \quad (\text{C1})$$

A similar formula holds for the gluon two-point function and the gluon regulator, which are invertible in the transverse subspace (see Eqs. (29), (46), (47)):

$$\left[\left(\frac{\delta^2 \Gamma_k}{\delta A \delta A} + R_{A,k} \right)^{-1} \right]_{ij, \mathbf{p}\mathbf{q}}^{ab} = \delta^{ab} t_{ij}(\mathbf{p}) G_{A,k}(p) (2\pi)^3 \delta^3(\mathbf{p} + \mathbf{q}) . \quad (\text{C2})$$

Therefore, the truncated gluon flow equation, Fig. 4, see also Eq. (B9), reduces to

$$\begin{aligned} 2\delta^{ab} t_{ij}(\mathbf{p}) \dot{\omega}_k(p) (2\pi)^3 \delta^3(\mathbf{p} + \mathbf{q}) = & \\ - \int \frac{d^3[p_{1\dots 6}]}{(2\pi)^{18}} \delta^{cd} \dot{\bar{R}}_{c,k}(p_1) (2\pi)^3 \delta^3(\mathbf{p}_1 - \mathbf{p}_2) \delta^{de} \bar{G}_{c,k}(p_2) (2\pi)^3 \delta^3(\mathbf{p}_2 - \mathbf{p}_3) & \\ \times f^{eaf} t_{im}(\mathbf{p}) (ip_{4,m}) (2\pi)^3 \delta^3(\mathbf{p} + \mathbf{p}_3 - \mathbf{p}_4) \delta^{fg} \bar{G}_{c,k}(p_4) (2\pi)^3 \delta^3(\mathbf{p}_4 - \mathbf{p}_5) & \\ \times f^{gbh} t_{jl}(\mathbf{q}) (ip_{6,l}) (2\pi)^3 \delta^3(\mathbf{q} + \mathbf{p}_5 - \mathbf{p}_6) \delta^{hc} \bar{G}_{c,k}(p_6) (2\pi)^3 \delta^3(\mathbf{p}_6 - \mathbf{p}_1) + (i \leftrightarrow j) , & \end{aligned} \quad (\text{C3})$$

and by carrying out index contractions and integrations we obtain the flow equation for ω_k :

$$\partial_t \omega_k(p) = -\frac{N_c}{2} \int \frac{d^3 q}{(2\pi)^3} \left(\bar{G}_{c,k} \dot{\bar{R}}_{c,k} \bar{G}_{c,k} \right) (q) \bar{G}_{c,k}(|\mathbf{p} + \mathbf{q}|) q^2 (1 - (\hat{\mathbf{p}} \cdot \hat{\mathbf{q}})^2) . \quad (\text{C4})$$

In much the same way we treat the truncated ghost flow equation, Fig. 5, see also Eq. (B8), to get

$$\begin{aligned} -\delta^{ab} \partial_t d_k^{-1}(p) (2\pi)^3 \delta^3(\mathbf{p} + \mathbf{q}) = & \\ \int \frac{d^3[p_{1\dots 6}]}{(2\pi)^{18}} \delta^{cd} t_{ij}(\mathbf{p}_1) \dot{R}_{A,k}(p_1) (2\pi)^3 \delta^3(\mathbf{p}_1 - \mathbf{p}_2) \delta^{de} t_{jh}(\mathbf{p}_2) G_{A,k}(p_2) (2\pi)^3 \delta^3(\mathbf{p}_2 - \mathbf{p}_3) & \\ \times f^{fea} t_{lh}(\mathbf{p}_3) (-ip_{4,l}) (2\pi)^3 \delta^3(\mathbf{p} + \mathbf{p}_3 - \mathbf{p}_4) \delta^{fg} \bar{G}_{c,k}(p_4) (2\pi)^3 \delta^3(\mathbf{p}_4 - \mathbf{p}_5) & \\ \times f^{bhg} t_{mn}(\mathbf{p}_6) (iq_m) (2\pi)^3 \delta^3(\mathbf{q} + \mathbf{p}_5 - \mathbf{p}_6) \delta^{hc} t_{ni}(\mathbf{p}_6) G_{A,k}(p_6) (2\pi)^3 \delta^3(\mathbf{p}_6 - \mathbf{p}_1) & \\ + \int \frac{d^3[p_{1\dots 6}]}{(2\pi)^{18}} \delta^{hc} \dot{\bar{R}}_{c,k}(p_1) (2\pi)^3 \delta^3(\mathbf{p}_1 - \mathbf{p}_2) \delta^{cd} \bar{G}_{c,k}(p_2) (2\pi)^3 \delta^3(\mathbf{p}_2 - \mathbf{p}_3) & \\ \times f^{bed} t_{mi}(\mathbf{p}_4) (iq_m) (2\pi)^3 \delta^3(\mathbf{q} + \mathbf{p}_3 - \mathbf{p}_4) \delta^{ef} t_{ij}(\mathbf{p}_4) G_{A,k}(p_4) (2\pi)^3 \delta^3(\mathbf{p}_4 - \mathbf{p}_5) & \\ \times f^{gfa} t_{hj}(\mathbf{p}_5) (-ip_{6,h}) (2\pi)^3 \delta^3(\mathbf{p} + \mathbf{p}_5 - \mathbf{p}_6) \delta^{gh} \bar{G}_{c,k}(p_6) (2\pi)^3 \delta^3(\mathbf{p}_6 - \mathbf{p}_1) , & \end{aligned} \quad (\text{C5})$$

which, after receiving the same treatment as the gluon equation above, finally turns into,

$$\begin{aligned} \partial_t d_k^{-1}(p) = N_c p^2 \int \frac{d^3 q}{(2\pi)^3} \left[\left(G_{A,k} \dot{R}_{A,k} G_{A,k} \right) (q) \bar{G}_{c,k}(|\mathbf{p} + \mathbf{q}|) (1 - (\hat{\mathbf{p}} \cdot \hat{\mathbf{q}})^2) \right. & \\ \left. + \left(\bar{G}_{c,k} \dot{R}_{c,k} \bar{G}_{c,k} \right) (q) G_{A,k}(|\mathbf{p} + \mathbf{q}|) q^2 \frac{1 - (\hat{\mathbf{p}} \cdot \hat{\mathbf{q}})^2}{(\mathbf{p} + \mathbf{q})^2} \right] . & \end{aligned} \quad (\text{C6})$$

Appendix D: Numerical Computation

Below we give some details of the numerical method used for the solution of the flow equations. In order to solve the flow equations numerically, the functions $\omega(p)$ and $d(p)$ of section IV C as well as $\omega_k(p)$ and $d_k(p)$ of section IV B are represented by means of Chebyshev polynomials on suitably sized momentum ranges, spanning up to nine orders of magnitude. We use a logarithmic momentum scale to sample the behavior of the functions equally well on all orders of magnitude; the function values are also represented logarithmically. In the case of the flow functions $\omega_k(p)$ and $d_k(p)$, which possess two momentum arguments, we first calculate the coefficients along the p -direction at constant values of k which are the Chebyshev nodes of the k -range, then determine the coefficients of the resulting functions in k -direction for each p -coefficient. About 130 Chebyshev nodes in each direction have been used. The momentum integrals, for the loop as well as for the flow (in section IV B), have been calculated using the Gauss-Legendre method with about 70 nodes. As for the Chebyshev nodes, the Gauss-Legendre nodes for the momentum integrals have been calculated for a logarithmic momentum scale in order to appropriately sample the IR behavior. The loop integrals have been confined to a range of one order of magnitude around the cutoff momentum k outside of which there is virtually no contribution to the integral, owing to the regulator functions employed, see Eq. (57).

In the loop integrals, the flow functions need to be evaluated also outside the Chebyshev representation range of the external momentum p . But the IR extrapolation of the flow functions requires no extra assumptions about their IR behavior: as long as k_{min} never reaches the lower boundary of the p -range, the functions can be simply chosen to be constant beyond this boundary, as clearly seen in Fig. 7. For their continuation in the UV, a power law has been fitted to their behavior in the UV region of the representation range, which is $\omega_k(p) \sim p$ and $d_k(p) \sim const.$ As for the k -range, the functions are never evaluated outside the Chebyshev range anyway, so no extrapolation is necessary.

The sets of equations (55), (56) as well as (61), (62) have been evaluated iteratively: starting from constant functions ω and d , the r.h.s. of the equations are calculated; from the result, the initial values of the flow, d_Λ and ω_Λ , are determined following the procedures de-

scribed in the next paragraph, giving temporary results ω^{tmp} , d^{tmp} . To improve the convergence behavior, we use a relaxation method to determine the final result of the n -th iteration as $\omega_k^{(n)}(p) = r\omega_k^{tmp}(p) + (1-r)\omega_k^{(n-1)}(p)$ for each Chebyshev node (k, p) , likewise for $d_k(p)$. Values of $r \in [0.1, 0.5]$ have been used, depending on how much the functions change from one iteration to the next. This yields the new functions $\omega^{(n)}$ and $d^{(n)}$ which are then fed back into the r.h.s. of the equations as input to the $(n+1)$ -th step of the iteration. This iteration is repeated until convergence is reached.

To determine the constant $d_\Lambda(p) \equiv d_\Lambda$ in Eq. (56), we demand that $d_{k_{min}}(p)$ fulfill a power law for p in the IR, $d_{k_{min}}^{-1}(p) \sim p^\beta$. To do so, we observe that for a power law $f(p) = p^\beta$, the expression

$$p \frac{d}{dp} \ln f(p) = \beta \quad (D1)$$

yields a constant value, i.e., the exponent. Let $g(p)$ be the r.h.s. of Eq. (56) (with $k = k_{min}$). We demand that

$$\frac{d}{dp} \left(p \frac{d}{dp} \ln (g(p) + d_\Lambda^{-1}) \right) \stackrel{!}{=} 0 \quad (D2)$$

and solve for d_Λ^{-1} . A least squares fit of a constant function to the expression obtained (which will in general not yet be constant) in the IR gives the optimal value for d_Λ^{-1} in order to achieve a power law behavior for $d_{k_{min}}^{-1}(p)$ in the IR region. This is done during each iteration step as described in the previous paragraph. In this way, we can impose a power law behavior on the ghost form factor without dictating its exponent. Concerning the Eqs. (55) (with $k = k_{min}$) and (62), we fit the expression $-a + bp$ to the r.h.s. in the UV and use $\omega_\Lambda(p) = a + p$ to achieve $\omega_{k=k_{min}}(p)|_{p \rightarrow \Lambda} \sim p$ for Eq. (55) and $\omega_0(p)|_{p \rightarrow \Lambda} \sim p$ for Eq. (62) which is an expression of asymptotic freedom. For Eq. (61) the determination of the initial conditions is not a numerical issue anyway, see Eq. (63).

This method allows for a systematic, simultaneous determination of the solution together with originally unknown initial conditions to accomplish that the solution at $k = k_{min}$ fulfill certain properties. Solving the differential equations in the differential form would require a trial-and-error search for the initial conditions to find a solution with the specified properties.

-
- [1] C. S. Fischer, A. Maas and J. M. Pawłowski, *Annals Phys.* **324** (2009) 2408 [arXiv:0810.1987 [hep-ph]].
 - [2] R. Alkofer and L. von Smekal, *Phys. Rept.* **353** (2001) 281 [arXiv:hep-ph/0007355].
 - [3] C. S. Fischer, *J. Phys. G* **32**, R253 (2006) [arXiv:hep-ph/0605173].
 - [4] L. von Smekal, arXiv:0812.0654 [hep-th].
 - [5] D. Binosi and J. Papavassiliou, *Phys. Rept.* **479** (2009)

- 1 [arXiv:0909.2536 [hep-ph]].
- [6] P. Boucaud, J. P. Leroy, A. Le Yaouanc, J. Micheli, O. Pene and J. Rodriguez-Quintero, *JHEP* **0806** (2008) 099 [arXiv:0803.2161 [hep-ph]].
- [7] D. F. Litim and J. M. Pawłowski, arXiv:hep-th/9901063.
- [8] J. M. Pawłowski, *Annals Phys.* **322** (2007) 2831 [arXiv:hep-th/0512261].
- [9] H. Gies, arXiv:hep-ph/0611146.

- [10] U. Ellwanger, M. Hirsch and A. Weber, Z. Phys. C **69** (1996) 687 [arXiv:hep-th/9506019].
- [11] D. Zwanziger, Nucl. Phys. B **518** (1998) 237.
L. Baulieu and D. Zwanziger, Nucl. Phys. B **548**, 527 (1999) [arXiv:hep-th/9807024].
- [12] P. Watson and H. Reinhardt, Phys. Rev. D **75**, 045021 (2007) [arXiv:hep-th/0612114].
P. Watson and H. Reinhardt, Phys. Rev. D **76**, 125016 (2007) [arXiv:0709.0140 [hep-th]].
P. Watson and H. Reinhardt, Phys. Rev. D **77**, 025030 (2008) [arXiv:0709.3963 [hep-th]].
- [13] R. Alkofer, A. Maas and D. Zwanziger, Few Body Syst. **47** (2010) 73 [arXiv:0905.4594 [hep-ph]].
- [14] A. P. Szczepaniak and E. S. Swanson, Phys. Rev. D **65**, 025012 (2002) [arXiv:hep-ph/0107078].
A. P. Szczepaniak, Phys. Rev. D **69**, 074031 (2004) [arXiv:hep-ph/0306030].
- [15] C. Feuchter and H. Reinhardt, Phys. Rev. D **70** (2004) 105021 [arXiv:hep-th/0408236], [arXiv:hep-th/0402106].
- [16] H. Reinhardt and C. Feuchter, Phys. Rev. D **71**, 105002 (2005) [arXiv:hep-th/0408237].
- [17] W. Schleifenbaum, M. Leder and H. Reinhardt, Phys. Rev. D **73**, 125019 (2006) [arXiv:hep-th/0605115].
- [18] D. Eppe, H. Reinhardt and W. Schleifenbaum, Phys. Rev. D **75**, 045011 (2007) [arXiv:hep-th/0612241].
- [19] D. Eppe, H. Reinhardt, W. Schleifenbaum and A. P. Szczepaniak, Phys. Rev. D **77**, 085007 (2008) [arXiv:0712.3694 [hep-th]].
- [20] H. Reinhardt, D. Campagnari, D. Eppe, M. Leder, M. Pak and W. Schleifenbaum, arXiv:0807.4635 [hep-th].
- [21] H. Reinhardt, Phys. Rev. Lett. **101** (2008) 061602 [arXiv:0803.0504 [hep-th]].
- [22] C. Wetterich, Phys. Lett. B **301** (1993) 90.
- [23] G. Burgio, M. Quandt and H. Reinhardt, Phys. Rev. D **81** (2010) 074502 [arXiv:0911.5101 [hep-lat]].
- [24] C. S. Fischer and J. M. Pawłowski, Phys. Rev. D **80** (2009) 025023 [arXiv:0903.2193 [hep-th]]; Phys. Rev. D **75** (2007) 025012 [arXiv:hep-th/0609009].
- [25] R. Alkofer, M. Q. Huber and K. Schwenzer, Phys. Rev. D **81** (2010) 105010 [arXiv:0801.2762 [hep-th]]; arXiv:0904.1873 [hep-th].
- [26] C. Lerche and L. von Smekal, Phys. Rev. D **65** (2002) 125006 [arXiv:hep-ph/0202194].
- [27] D. Campagnari, A. Weber, H. Reinhardt, F. Astorga and W. Schleifenbaum, arXiv:0910.4548 [hep-th].
- [28] D. Zwanziger, Nucl. Phys. **B364**, 127 (1991); Nucl. Phys. **B485**, 185 (1997); Phys. Rev. D **70**, 094034 (2004).
- [29] J. C. Taylor, Nucl. Phys. **B33**, 436 (1971); W. Marciano and H. Pagels, Phys. Rept. **36**, 137 (1978).
- [30] A. Cucchieri, T. Mendes and A. Mihara, JHEP **12**, 012 (2004); A. Sternbeck, E. M. Ilgenfritz, M. Müller-Preussker and A. Schiller, Nucl. Phys. B Proc. Suppl. **153**, 185 (2006).
- [31] D. Campagnari, H. Reinhardt and A. Weber, Phys. Rev. D **80**, 025005 (2009) [arXiv:0904.3490 [hep-th]].
- [32] C. S. Fischer and D. Zwanziger, Phys. Rev. D **72** (2005) 054005 [arXiv:hep-ph/0504244].
- [33] U. Ellwanger, Phys. Lett. B **335** (1994) 364.
- [34] F. Freire, D. F. Litim and J. M. Pawłowski, Phys. Lett. B **495** (2000) 256 [arXiv:hep-th/0009110].
- [35] J. M. Pawłowski, in preparation.
- [36] J. M. Pawłowski, D. F. Litim, S. Nedelko and L. von Smekal, Phys. Rev. Lett. **93** (2004) 152002 [arXiv:hep-th/0312324].
- [37] D. F. Litim, Phys. Lett. B **486** (2000) 92; Int. J. Mod. Phys. A **16** (2001) 2081.
- [38] J. Braun, H. Gies and J. M. Pawłowski, Phys. Lett. B **684** (2010) 262 [arXiv:0708.2413 [hep-th]].
- [39] J. Braun, L. M. Haas, F. Marhauser and J. M. Pawłowski, arXiv:0908.0008 [hep-ph].